PHYSICAL REVIEW B **94**, 220303(R) (2016)

Boron arsenide phonon dispersion from inelastic x-ray scattering: Potential for ultrahigh thermal conductivity

Hao Ma,[1] Chen Li,[1] Shixiong Tang,[1] Jiaqiang Yan,[2,3] Ahmet Alatas,[4] Lucas Lindsay,[2] Brian C. Sales,[2] and Zhiting Tian[1,*]

[1]*Department of Mechanical Engineering, Virginia Tech, Blacksburg, Virginia 24061, USA*

[2]*Materials Science and Technology Division, Oak Ridge National Laboratory, Oak Ridge, Tennessee 37831, USA*

[3]*Department of Materials Science and Engineering, University of Tennessee, Knoxville, Tennessee 37996, USA*

[4]*Advanced Photon Source, Argonne National Laboratory, Argonne, Illinois 64039, USA*

(Received 16 August 2016; published 14 December 2016)

Cubic boron arsenide (BAs) was predicted to have an exceptionally high thermal conductivity (k) $\sim$ 2000 $\mathrm{W\,m^{-1}K^{-1}}$ at room temperature, comparable to that of diamond, based on first-principles calculations. Subsequent experimental measurements, however, only obtained a k of $\sim$200 $\mathrm{W\,m^{-1}K^{-1}}$. To gain insight into this discrepancy, we measured phonon dispersion of single-crystal BAs along high symmetry directions using inelastic x-ray scattering and compared these with first-principles calculations. Based on the measured phonon dispersion, we have validated the theoretical prediction of a large frequency gap between acoustic and optical modes and bunching of acoustic branches, which were considered the main reasons for the predicted ultrahigh k. This supports its potential to be a super thermal conductor if very-high-quality single-crystal samples can be synthesized.

DOI: 10.1103/PhysRevB.94.220303

I. INTRODUCTION

As the electronics industry expands rapidly and chip fabrication technology evolves towards further miniaturization, power density and heat flux increase steeply [1,2]. Thermal management becomes a critical bottleneck for the advancement of a variety of important defense, space, and commercial applications. Engineers have been hunting for ways to cool chips. Developing energy-efficient thermal management technologies is a key to energy saving. Thus, the ability to identify and understand materials with high thermal conductivities is increasingly important. The highest thermal conductivities of any bulk materials at room temperature are found in carbon-based materials, diamond and graphite. However, diamond is scarce, and suffers growth difficulties [3]. Thus, it is appealing to identify alternate materials with ultrahigh thermal conductivities derived from fundamentally different lattice dynamical properties.

Cubic boron arsenide (BAs) was predicted to have a remarkable lattice thermal conductivity (k) over 2000 $\mathrm{Wm^{-1}K^{-1}}$ at room temperature based on first-principles calculations [4,5]. This is comparable to the highest bulk k values known. The exceptionally high k from these calculations was attributed to reduced phonon-phonon scattering due to a large acoustic-optical phonon frequency gap and bunching of the acoustic branches, based on calculated phonon dispersion curves. While a previous Raman experiment showed some indication of a large frequency gap in BAs [6], direct experimental evidence of this feature or acoustic bunching is missing, thus validation of the phonon features from which the predicted high k is derived has not been possible. Inspired by the ultrahigh-k prediction, a recent measurement obtained $k \sim 200\ \mathrm{Wm^{-1}K^{-1}}$ [7,8], an order of magnitude lower than the predicted value. Lack of measured dispersion data coupled with the large discrepancy of calculated and measured k values begs the question, is this k discrepancy due to extrinsic scattering mechanisms as hypothesized in Ref. [6] or from inaccurately calculated phonon dispersion data?

In this Rapid Communication, we measure the phonon dispersion of BAs along high symmetry directions using inelastic x-ray scattering (IXS) and compare with first-principles calculations. While Raman or Brillouin scattering can only probe zone center optical modes, IXS and inelastic neutron scattering (INS) are powerful tools to investigate phonon dispersion relations throughout the Brillouin zone, both acoustic and optical. As a result of high flux and high brilliance of modern x-ray sources, IXS has the ability to probe much smaller samples than are accessible to INS [9,10]. INS experiments require sample volumes typically of several $\mathrm{mm^3}$, while IXS measurements can be performed on samples with volumes several orders of magnitude smaller. This opens up possibilities to study materials only available in very small quantities, as is the case here for BAs where high-quality large single-crystal growth is challenging. IXS has been applied to study phonon dispersions and linewidths of several low-k materials, such as $PbTe_{1-x}Se_x$ [11], $TiSe_2$ [12], TiO_2 [13], VO_2 [14], MgB_2 [15], and URu_2Si_2 [16]. Phonon dispersions of high-k materials, such as graphite [17], have also been determined by IXS. We provide direct experimental confirmation of the large acoustic-optical frequency gap and acoustic bunching in BAs, and find good agreement between measured and calculated dispersion data.

II. CRYSTAL GROWTH AND CHARACTERIZATION

Single crystals of cubic BAs were grown at Oak Ridge National Laboratory by a vapor transport technique with iodine as the transport agent. The starting materials were B powder and As chunks. In a typical growth process, B and As in an atomic ratio of 1:1.15 were loaded into a well-cleaned quartz tube with an inner diameter of 16 mm and a length of 120 cm. After adding 0.4 g of I_2, the quartz tube was sealed under

*Corresponding author: zhiting@vt.edu

vacuum. The sealed ampoule was heated to 650°C for 36 h, kept for 48 h, and then heated to 900°C for 15 h. The growth was performed for 12 days with the cold end at 850°C. The presence of extra As has been found to increase the growth rate as reported before [18], which signals the importance of AsI_3 in the vapor transport growth of BAs.

X-ray powder diffraction on pulverized single crystals was performed on a PANalytical X'Pert Pro MPD powder x-ray diffractometer using Cu $K\alpha_1$ radiation. No impurity peaks were observed. Elemental analysis of the crystals was performed using a Hitachi TM-3000 tabletop electron microscope equipped with a Bruker Quantax 70 energy dispersive x-ray (EDX) system. Within the resolution of the instrument the elemental analysis confirmed the composition to be stoichiometric cubic BAs.

Before performing IXS experiments, we did single-crystal x-ray diffraction (XRD) measurements to identify the number of domains and their relative ratio. The BAs crystal ($20 \times 90 \times 160$ μm^3) was centered on the goniometer of a Rigaku Oxford Diffraction Gemini E Ultra single-crystal diffractometer operating with Mo $K\alpha$ radiation and equipped with a 0.5 mm diameter collimator. The data collection routine, unit cell determination, and data integration were carried out with the program CRYSALISPRO [19]. A data set was collected to 0.7 Å resolution and covering enough of reciprocal space under $\bar{4}3m$ Laue symmetry to ensure a complete data set for all domains present.

A preliminary search of the raw data images was done to identify positions of the stronger diffraction peaks. A total of 134 peaks were identified. Figure 1(a) displays the result of the preliminary search. As the preliminary peak search only identifies the strongest peaks of two major domains and cannot determine the ratio of the intensity contributions to the two domains, especially for the overlapped peaks, the preliminary cell determination is only useful for identifying the number of significant domains, but not the relative size of the domains. To do this, the intensities of the spots from the two domains were integrated in CRYSALISPRO using an automatic software routine. The relative ratios of the two domains were determined to be 95% and 5%. The two domains were twinned by an 180° rotation around the [111] axis. This crystal twinning was also found in the BAs samples used in previous k measurements [7]. Large single-crystal growth of boron-related materials is known to be challenging and the high volatility and toxicity of As adds further complexity to the process [20,21]. The XRD pattern of crystal BAs is shown in Fig. 1(b).

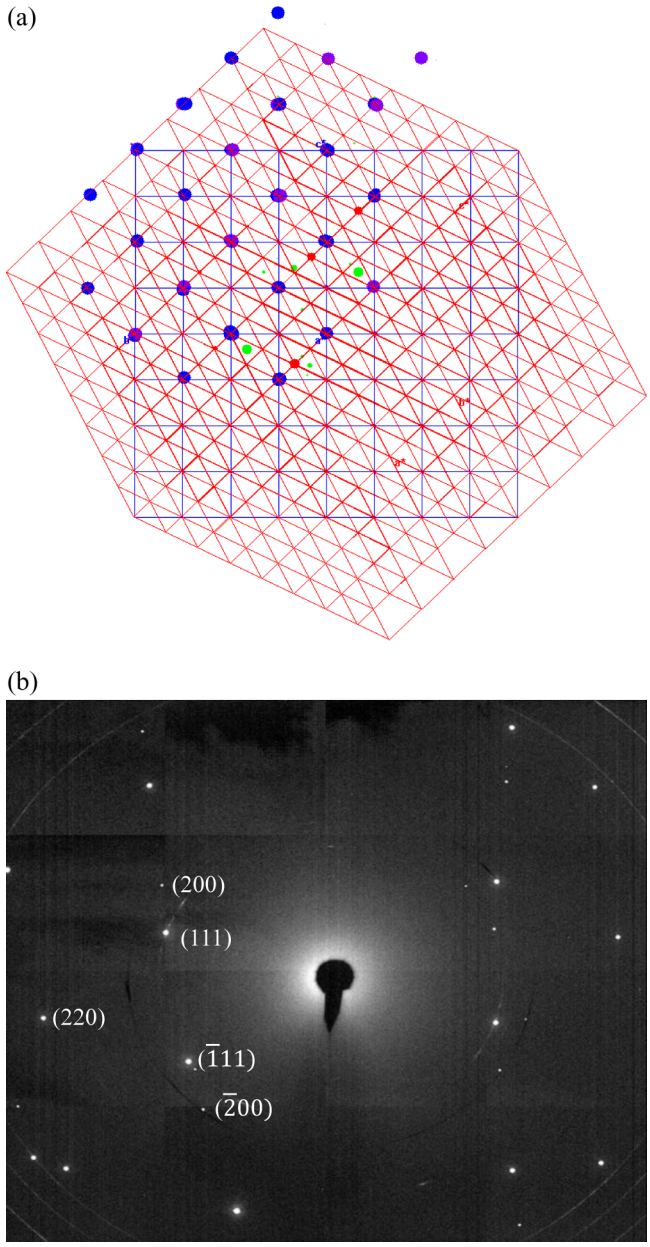

FIG. 1. (a) Image overlaying the reciprocal lattice and the diffraction peak positions of the two domains identified in our BAs crystal. The spot sizes are roughly scaled to the spot intensity. The blue lattice and spots represent the largest domain. The red lattice and spots represent the second largest domain. A total of 58 peaks fit *only* the major (blue) domain, and 17 peaks fit *only* the minor (red) domain. A total of 27 (purple) fit both domains. Green spots (32 total; almost all weak) do not fit either of the blue or red domains, and suggest the presence of one or more minor domains that could not be identified. (b) XRD pattern of BAs crystal. The BAs crystal was rotating during long exposure to x ray.

III. INELASTIC X-RAY SCATTERING

We performed the IXS measurements at room temperature at the XOR 3-ID HERIX beam line of the Advanced Photon Source, Argonne National Laboratory. The synchrotron-based IXS technique provides high energy resolution and can probe phonon properties via energy and momentum changes of the scattered photon [11,22–24]. The wavelength of the x ray is 0.5725 Å and the focused beam size is 10 μm × 10 μm. The experiment was carried out in transmission geometry. Figure 2 gives a typical IXS spectrum characterized by an elastic peak centered at zero energy and an inelastic peak associated with the creation of a phonon. Due to limited beam time we did not measure the negative energy peak (phonon annihilation). To reduce statistical noise, we measured multiple runs and averaged the data for each q point sampled. The instrument resolution was measured separately. The energy resolution of 2.0 meV was determined by the full width at half maximum (FWHM) of a pseudo-Voigt function. The phonon frequencies

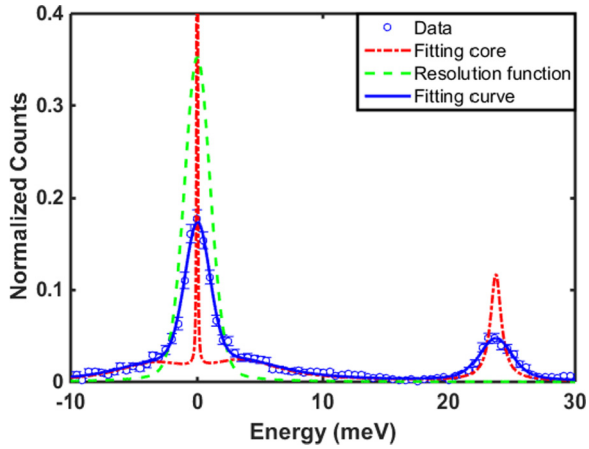

FIG. 2. Energy spectra from IXS measurement (blue circles) of the (0.2, 0.2, 0.2) longitudinal acoustic (LA) mode. Green and red curves represent the resolution function and model function, respectively. The blue solid curve denotes the convolution between the resolution function and fitting core.

were obtained by fitting data with a Lorentzian model. The momentum resolution was 0.7 nm^{-1}. After fitting each q point, we obtained the mode dependent phonon frequencies.

IV. RESULTS AND DISCUSSION

As shown in Fig. 3, our IXS data matches well with previous density functional perturbation theory (DFPT) calculations [4,5]. Raman data for Γ-point optical phonons [25] are also included. The ultrahigh k of cubic BAs was attributed to limited intrinsic resistance from three-phonon scatterings governed by (1) a large frequency gap between the acoustic and optical phonons and (2) bunching of the acoustic branches [5]. These dispersion features limit the phase space for three-phonon scatterings dictated by conservation of energy and momentum conditions. The frequency gap prohibits two acoustic

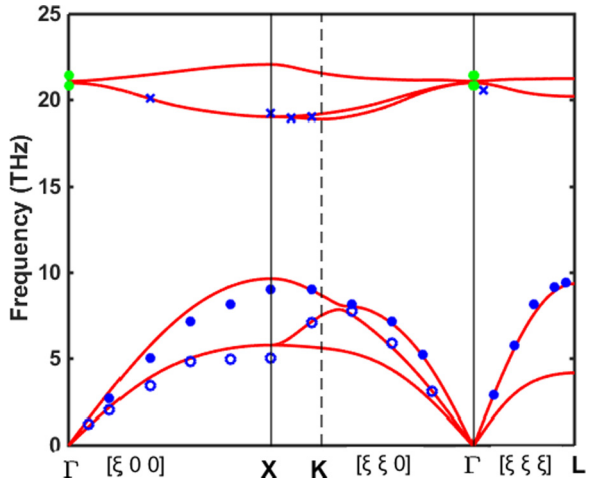

FIG. 3. Bottom: Experimental (markers) and theoretical (solid lines) [5] phonon dispersion of BAs. Green circle makers are Raman data [25]. Solid markers are for LA modes and open ones are for TA modes.

phonons from scattering with an optical phonon and acoustic bunching limits the phase space for three acoustic phonon scatterings, especially important for higher frequency acoustic modes.

Based on our measured phonon dispersion, a large acoustic-optical phonon frequency gap and bunching of the acoustic branches, on which the prediction of ultrahigh k depends, are confirmed experimentally. Also, this agreement between calculated and measured dispersions further validates the predictive power of first-principles calculations of vibrational properties of materials.

Unfortunately, the existence of two major domains in our BAs sample prohibits confident measurement of frequencies of the transverse acoustic (TA) modes in the [111] direction and the lower TA branch in the [110] direction. Attempts were made to measure the lower TA branch in the [110] direction for q points (0.05 0.05 0), (0.1 0.1 0), and (0.2 0.2 0). With decreasing q magnitude phonon frequencies are expected to decrease and approach zero near the Γ point. The measurements for these points gave nearly constant behavior with 3.76, 3.60, and 3.30 THz, respectively. Using three different zones for the frequency measurements of these points gave similar behavior. This suggests that these measured frequency data assumed for q points in domain I could actually come from q points in domain II. To confirm this, we calculated the corresponding q points of domain II and they are (0.34 −0.95 −0.77), (0.4 − 0.07 − 0.27), and (0.4 − 0.14 − 0.28). Then, we calculated the acoustic phonon frequencies of these three points using DFPT. The experimental data are close to the lowest acoustic modes calculated for the three q points in domain II with frequencies of 3.59, 4.02, and 4.05 THz, respectively. In other words, as a result of crystal twinning, the phonon modes in domain II mask the phonon modes in domain I along certain directions and thus prevent us from determining the lower TA branch in the [110] direction and TA branches in the [111] direction.

V. SUMMARY

We measured phonon dispersion of cubic BAs by inelastic x-ray scattering and observed good agreement between our measurements and first-principles calculations for phonon dispersions. This work provides direct experimental confirmation of the two phonon dispersion features responsible for the predicted high k of this system: (1) bunching of the acoustic branches and (2) a large acoustic-optical frequency gap. This demonstrates again the predictive power of first-principles DFPT calculations for determining phonon dispersions. As a direct and detailed comparison between experiment and calculation on phonon properties of BAs, our work serves as a crucial step towards the search for unconventional materials with ultrahigh k for microelectronic cooling.

ACKNOWLEDGMENTS

This work was funded by the startup fund from Virginia Polytechnic Institute and State University. We thank Dr. Carla Slebodnick at Virginia Tech for her help with single-crystal x-ray diffraction measurements. We are grateful for useful

discussions with Dr. David Broido at Boston College. L.L., J.-Q.Y., and B.C.S. acknowledge support from the U.S. Department of Energy, Office of Science, Office of Basic Energy Sciences, Materials Sciences and Engineering Division. This research used resources of the Advanced Photon Source, a U.S. Department of Energy (DOE) Office of Science User Facility operated for the DOE Office of Science by Argonne National Laboratory under Contract No. DE-AC02-06CH11357.

[1] P. Ball, Computer engineering: Feeling the heat, Nature (London) **492**, 174 (2012).

[2] S. V. Garimella, L.-T. Yeh, and T. Persoons, Thermal management challenges in telecommunication systems and data centers, IEEE Trans. Compon., Packag., Manuf. Technol. **2**, 1307 (2012).

[3] Graphite has weak interlayer van der Waals bonding which makes it highly anisotropic and the material mechanically soft, and thus is not appropriate for many applications.

[4] L. Lindsay, D. A. Broido, and T. L. Reinecke, First-Principles Determination of Ultrahigh Thermal Conductivity of Boron Arsenide: A Competitor for Diamond? Phys. Rev. Lett. **111**, 025901 (2013).

[5] D. A. Broido, L. Lindsay, and T. L. Reinecke, *Ab initio* study of the unusual thermal transport properties of boron arsenide and related materials, Phys. Rev. B **88**, 214303 (2013).

[6] V. G. Hadjiev, M. N. Iliev, B. Lv, Z. F. Ren, and C. W. Chu, Anomalous vibrational properties of cubic boron arsenide, Phys. Rev. B **89**, 024308 (2014).

[7] B. Lv *et al.*, Experimental study of the proposed super-thermal-conductor: BAs, Appl. Phys. Lett. **106**, 074105 (2015).

[8] J. Kim *et al.*, Thermal and thermoelectric transport measurements of an individual boron arsenide microstructure, Appl. Phys. Lett. **108**, 201905 (2016).

[9] M. Krisch and F. Sette, Inelastic x-ray scattering from phonons, in *Light Scattering in Solids IX*, edited by M. Cardona and R. Merlin (Springer, Berlin, 2007), pp. 317–370.

[10] B. Eberhard, Phonon spectroscopy by inelastic x-ray scattering, Rep. Prog. Phys. **63**, 171 (2000).

[11] Z. T. Tian *et al.*, Inelastic x-ray scattering measurements of phonon dispersion and lifetimes in $PbTe_{1-x}Se_x$ alloys, J. Phys.: Condens. Matter **27**, 375403 (2015).

[12] F. Weber, S. Rosenkranz, J.-P. Castellan, R. Osborn, G. Karapetrov, R. Hott, R. Heid, K.-P. Bohnen, and A. Alatas, Electron-Phonon Coupling and the Soft Phonon Mode in $TiSe_2$, Phys. Rev. Lett. **107**, 266401 (2011).

[13] B. Wehinger, A. Bosak, and P. T. Jochym, Soft phonon modes in rutileTiO_2, Phys. Rev. B **93**, 014303 (2016).

[14] J. D. Budai *et al.*, Metallization of vanadium dioxide driven by large phonon entropy, Nature (London) **515**, 535 (2014).

[15] A. Shukla *et al.*, Phonon Dispersion and Lifetimes in MgB_2, Phys. Rev. Lett. **90**, 095506 (2003).

[16] D. R. Gardner, C. J. Bonnoit, R. Chisnell, A. H. Said, B. M. Leu, T. J. Williams, G. M. Luke, and Y. S. Lee, Inelastic x-ray scattering measurements of phonon dynamics in URu_2Si_2, Phys. Rev. B **93**, 075123 (2016).

[17] M. Mohr, J. Maultzsch, E. Dobardžić, S. Reich, I. Milošević, M. Damnjanović, A. Bosak, M. Krisch, and C. Thomsen, Phonon dispersion of graphite by inelastic x-ray scattering, Phys. Rev. B **76**, 035439 (2007).

[18] T. L. Chu and A. E. Hyslop, Crystal growth and properties of boron monoarsenide, J. Appl. Phys. **43**, 276 (1972).

[19] CRYSALISPRO Software System, v., Rigaku Oxford Diffraction, 2015, Rigaku Corporation, Oxford, U.K.

[20] S. Wang *et al.*, Synthesis and characterization of a *p*-type boron arsenide photoelectrode, J. Am. Chem. Soc. **134**, 11056 (2012).

[21] F. V. Williams and R. A. Ruehrwein, The preparation and properties of boron phosphides and arsenides, J. Am. Chem. Soc. **82**, 1330 (1960).

[22] H. Sinn *et al.*, An inelastic x-ray spectrometer with 2.2 meV energy resolution, Nucl. Instrum. Methods Phys. Res., Sect. A **467-468**, 1545 (2001).

[23] T. S. Toellner, A. Alatas, and A. H. Said, Six-reflection meV-monochromator for synchrotron radiation, J. Synchrotron Radiat. **18**, 605 (2011).

[24] A. Alatas *et al.*, Improved focusing capability for inelastic x-ray spectrometer at 3-ID of the APS: A combination of toroidal and Kirkpatrick-Baez (KB) mirrors, Nucl. Instrum. Methods Phys. Res., Sect. A **649**, 166 (2011).

[25] R. G. Greene, H. Luo, A. L. Ruoff, S. S. Trail, and F. J. DiSalvo, Jr., Pressure Induced Metastable Amorphization of BAs: Evidence for a Kinetically Frustrated Phase Transformation, Phys. Rev. Lett. **73**, 2476 (1994).